EMBO reports

scientific report

Rmi1, a member of the Sgs1–Top3 complex in budding yeast, contributes to sister chromatid cohesion

Mong Sing Lai[1], *Masayuki Seki*[1+], *Ayako Ui*[1] *& Takemi Enomoto*[1,2]

[1]Molecular Cell Biology Laboratory, Graduate School of Pharmaceutical Sciences, Tohoku University, Sendai, Miyagi, Japan, and [2]Tohoku University 21st Century COE Program, 'Comprehensive Research and Education Center for Planning of Drug Development and Clinical Evaluation', Sendai, Miyagi, Japan

The *Saccharomyces cerevisiae* RecQ-mediated genome instability (Rmi1) protein was recently identified as the third member of the slow growth suppressor 1–DNA topoisomerase III (Sgs1–Top3) complex, which is required for maintaining genomic stability. Here, we show that cells lacking *RMI1* have a mitotic delay, which is partly dependent on the spindle checkpoint, and are sensitive to the microtubule depolymerizing agent benomyl. We show that *rmi1* and *top3* single mutants are defective in sister chromatid cohesion, and that deletion of *SGS1* suppresses benomyl sensitivity and the cohesion defect in these mutant cells. Loss of *RAD51* also suppresses the cohesion defect of *rmi1* mutant cells. These results indicate the existence of a new pathway involving Rad51 and Sgs1-Top3-Rmi1, which leads to the establishment of sister chromatid cohesion.

Keywords: DNA replication; sister chromatid cohesion; Sgs1; Rmi1; Top3

EMBO reports (2007) **8**, 685–690. doi:10.1038/sj.embor.7401000

INTRODUCTION

The RecQ family of DNA helicases has important roles in the maintenance of genomic integrity. In humans, five genes encoding the RecQ family of DNA helicases—*RECQL1*, *BLM*, *WRN*, *RECQL4* and *RECQL5*—have been identified, and defects in three—*BLM*, *WRN* and *RECQL4*—cause Bloom syndrome, Werner syndrome and Rothmund–Thomson syndrome, respectively; all these disorders are associated with genomic instability (Ellis *et al*, 1995; Yu *et al*, 1996; Kitao *et al*, 1999). In the budding yeast *Saccharomyces cerevisiae*, only a single gene encodes the RecQ family DNA helicase slow growth suppressor 1 (*SGS1*), and cells lacking *SGS1* show phenotypes similar to those observed in cells from patients with Bloom syndrome and Werner syndrome, including hyper-recombination (Watt *et al*, 1996).

A mutant allele of *SGS1* was identified as a suppressor of the slow-growth phenotype of the DNA topoisomerase III (*TOP3*) mutant (Gangloff *et al*, 1994), and Sgs1 interacts physically with Top3 (Bennett *et al*, 2000). Sgs1 and Top3 are required for damage-induced recombination repair (Ui *et al*, 2001, 2005), and are thought to be involved in the resolution of recombination intermediates (Ira *et al*, 2003). RecQ-mediated genome instability (*RMI1*) was identified as the third member of the Sgs1–Top3 complex, and cells lacking *SGS1*, *TOP3* or *RMI1* show slow growth, poor sporulation, genome instability and hyper-recombination (Chang *et al*, 2005; Mullen *et al*, 2005). In addition, *sgs1* and *rmi1* mutant cells show the same range of synthetic lethality/sickness interactions with *rrm3*, *slx1*, *slx4*, *mus81* and *mms4* mutations (Tong *et al*, 2004). Analyses of the synthetic lethality between *sgs1* and the above mutations showed that the Sgs1–Top3–Rmi1 complex seems to function in the repair or bypass of spontaneous S-phase damage (Fabre *et al*, 2002; Fricke & Brill, 2003; Schmidt & Kolodner, 2004; Torres *et al*, 2004).

Accurate transmission of chromosomes to daughter cells is important for the maintenance of genomic integrity. It is well known that sister chromatid cohesion—the physical association of replicated sister chromatids—has an important role in the precise segregation of chromosomes, thereby ensuring high-fidelity chromosome transmission (Koshland & Guacci, 2000; Nasmyth *et al*, 2000). The cohesion of sister chromatids is mediated by a cohesin complex consisting of Smc1, Smc3, Scc1 and Scc3, and its establishment is coupled with DNA replication (Uhlmann, 2004). A screen for noncohesin components involved in sister chromatid cohesion identified several proteins involved in the DNA-damage response (Warren *et al*, 2004). It has also been reported that cohesin is recruited to sites of double-strand breaks during G2 (Strom *et al*, 2004). Here, we present a new finding that Rmi1 and Top3 function in sister chromatid cohesion downstream of Sgs1 in a pathway involving Rad51.

[1]Molecular Cell Biology Laboratory, Graduate School of Pharmaceutical Sciences, Tohoku University, Aoba 6-3, Aramaki, Aoba-Ku, Sendai, Miyagi 980-8578, Japan
[2]Tohoku University 21st Century COE Program, 'Comprehensive Research and Education Center for Planning of Drug Development and Clinical Evaluation', Aoba 6-3, Aramaki, Aoba-Ku, Sendai, Miyagi 980-8578, Japan
[+]Corresponding author. Tel: +81 22 795 6875; Fax: +81 22 795 6873;
E-mail: seki@mail.pharm.tohoku.ac.jp

Received 2 November 2006; revised 24 April 2007; accepted 25 April 2007; published online 15 June 2007

RESULTS AND DISCUSSION

G2/M delay in *rmi1* cells depends on the spindle checkpoint

Previous work has shown that cells lacking *RMI1* show slow growth and a large-budded morphology (Chang *et al*, 2005; Mullen *et al*, 2005). To determine whether the slow growth phenotype of *rmi1* mutant cells was accompanied by a specific defect in cell-cycle progression, we examined the cells by using flow cytometry. Consistent with previous reports, we found that, after release from α-factor, synchronous cultures of *rmi1* cells passed through G1 and S phase, and remained blocked in G2/M phase until the end of the experiment (240 min; Fig 1A). Microscopy analysis of asynchronous *rmi1* cells also showed an increase in the percentage of large-budded cells, with the nucleus located at or beyond the mother-bud neck, a morphology characteristic of the G2/M phase (Fig 1B). When we examined spindle morphology, we found that a higher proportion of *rmi1* cells had intermediate-length spindles compared with wild-type cells, suggesting that *rmi1* cells arrested at metaphase (supplementary Fig S1 online). In addition, a marked increase in the number of cells with aberrant spindle structures was observed in the *rmi1* mutant cell population (supplementary Fig S1 online).

Generally, mitotic delays could reflect activation of either the DNA-damage checkpoint (Weinert & Hartwell, 1988) or the mitotic spindle checkpoint (Li & Murray, 1991). Chang *et al* (2005) reported that the Rad53-dependent DNA-damage checkpoint is activated in *rmi1* cells. Therefore, we examined whether the accumulation of *rmi1* cells in G2/M phase was due to the activation of the mitotic arrest-deficient 2 (Mad2)-dependent spindle checkpoint. Flow cytometry analysis showed that the accumulation of *rmi1* cells in G2/M phase was partly suppressed by deletion of *MAD2* (Fig 1A). In addition, the percentage of large-budded cells with the nucleus located at or beyond the mother-bud neck, which was increased in *rmi1* cells, was also partly reduced by the deletion of *MAD2* (Fig 1C). The activation of the Mad2–spindle checkpoint stabilizes securin (Pds1) by inhibiting anaphase promoting complex (APC); therefore, we monitored levels of Pds1 throughout the cell cycle and found that Pds1 persisted for a long time in *rmi1* cells (supplementary Fig S2 online). These results indicate that the absence of *RMI1* activates the Mad2–spindle checkpoint, resulting in a delay in the progression of M phase.

Defective sister chromatid cohesion in *rmi1* and *top3* cells

The spindle checkpoint is required for correct chromosome segregation (Li & Murray, 1991). We were interested in whether Rmi1 was involved in some aspect of chromosome segregation as the mitotic spindle checkpoint was activated in *rmi1* cells. To assess the sensitivity of *rmi1* cells to perturbation of the chromosome segregation machinery, we exposed them to benomyl, a microtubule-depolymerizing drug. As shown in Fig 2A, *rmi1* cells were moderately sensitive to benomyl, compared with wild-type cells.

It has been shown that chromosome transmission fidelity (CTF) *ctf7* and *ctf18* mutant cells, which have defects in sister chromatid cohesion (Skibbens *et al*, 1999; Hanna *et al*, 2001; Mayer *et al*, 2001), show *MAD2*-dependent M-phase arrest and have intermediate-length spindles. As *rmi1* cells showed a similar phenotype to *ctf7* and *ctf18* mutants, we next tested whether Rmi1 has a role in sister chromatid cohesion.

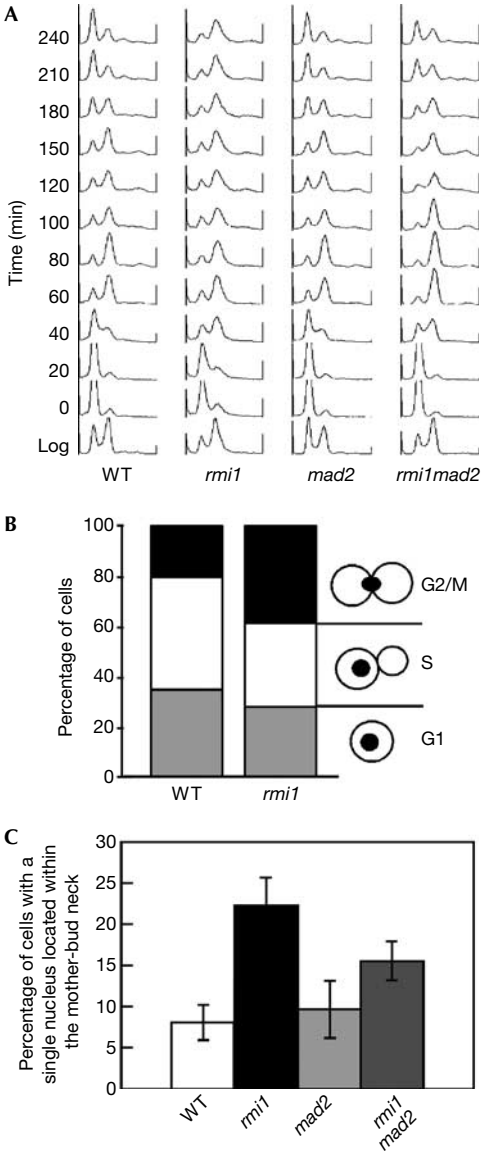

Fig 1 | Deletion of *RMI1* results in a G2/M-phase delay that is partly dependent on the mitotic spindle checkpoint. (**A**) Log-phase cultures of wild-type (WT; YK402a), *rmi1* (YK402ar1), *mad2* (YK402am2) and *rmi1mad2* (YK402ar1m2) cells were arrested with α-factor, released into YPD and processed for flow cytometry. (**B**) Log-phase cultures of wild-type (WT; yMP10381) and *rmi1* (SCRr1) cells were fixed with ethanol and stained with DAPI to visualize the DNA. Cells with no bud (G1), cells with bud (S) and large-budded cells with a single nucleus located within the mother-bud neck (G2/M) were scored. (**C**) Log-phase cultures of wild-type (WT; YK402a), *rmi1* (YK402ar1), *mad2* (YK402am2) and *rmi1mad2* (YK402ar1m2) cells were fixed with ethanol and stained with DAPI to visualize the DNA. Large-budded cells with a single nucleus located within the mother-bud neck were scored. The data shown represent the average of two independent experiments. One hundred cells were counted in each experiment. Bars indicate standard deviation. DAPI, 4,6-diamidino-2-phenylindole.

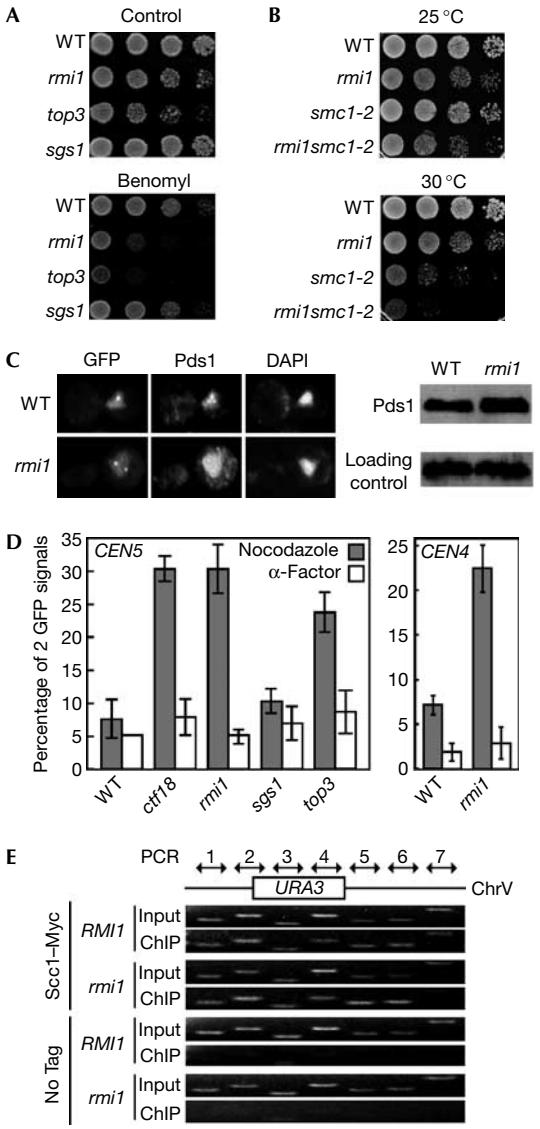

Fig 2 | *rmi1* and *top3* mutants are sensitive to benomyl and defective in sister chromatid cohesion. (**A**) Serial tenfold dilutions of log-phase cultures of wild-type (YPH1477), *rmi1* (YPH1477r1), *top3* (YPH1477t3) and *sgs1* (YPH1477s1) cells were spotted onto growth plates with or without 20 μg/ml benomyl, incubated at 30 °C for 3 days and then photographed. (**B**) Serial tenfold dilutions of log phase cultures of wild-type (982-6a), *rmi1* (982-6ar1), *smc1-2* (1355-1a) and *rmi1smc1-2* (1355-1ar1) cells were spotted onto growth plates, incubated at 25 °C (top) or 30 °C (bottom) for 3 days and then photographed. (**C**) Fluorescence micrographs of wild-type (YPH1477) and *rmi1* (YPH1477r1) cells showing GFP loci on sister chromatids (GFP), Pds1 and DNA (DAPI) (left panels). Cells expressing Pds1–13Myc in wild-type (YPH1477b1) or *rmi1* (YPH1477b1r1) cells were arrested in M phase (15 μg/ml nocodazole for 5 h) and analysed by western blotting (right panels). Histone H3 was used as a loading control. Pds1–13Myc and histone H3 were detected using Myc (9E10) monoclonal antibody and histone H3 antibody, respectively. (**D**) Wild-type (YPH1477; tet operator locus located 35 kb from *CEN5*), *ctf18* (YPH1477c18), *rmi1* (YPH1477r1), *sgs1* (YPH1477s1) and *top3* (YPH1477t3) cells (left panel) and wild-type (Y819; tet operator locus located 12.7 kb from *CEN4*) and *rmi1* (Y819r1) cells (right panel) were arrested in M-phase with nocodazole or in G1-phase with α-factor and then fixed with paraformaldehyde. One hundred cells of each strain were scored for the number of cells with two GFP signal foci. The data shown represent the average of three experiments. Bars indicate standard deviation. (**E**) Chromatin immunoprecipitation (ChIP) analysis at the *URA3* locus. Seven PCR products designed to span the *URA3* locus are shown (Lam *et al*, 2006). Scc1–13Myc ChIP was carried out in the presence (YK402aSCC1) or absence (YK402aSCC1r1) of *RMI1*. Cells were arrested in M-phase (15 μg/ml nocodazole for 5 h) before proceeding with ChIP. Input is the chromatin solution used to perform ChIP. A no-tag control is shown for each experiment. ChrV, chromosome 5; DAPI, 4,6-diamidino-2-phenylindole; GFP, green fluorescent protein; WT, wild-type.

First, we assessed the genetic interactions between *RMI1* and *SMC1*—a gene that functions in sister chromatid cohesion, the conditional allele (*smc1-2*) of which confers a synthetically lethal phenotype in the absence of *CTF8* (Mayer *et al*, 2001). We observed conditional synthetic sickness between *rmi1* and *smc1–2*, suggesting that *RMI1* is involved in cohesion (Fig 2B).

Next, we assessed cohesion directly by using cells that were constructed as described previously (Michaelis *et al* 1997). When arrested in M phase with nocodazole, wild-type cells showed one green fluorescent protein (GFP) signal, which is indicative of nonseparated sister chromatids, whereas mutants defective in cohesion showed two GFP signal foci, which is indicative of separated sister chromatids (Fig 2C). We compared the efficiency of sister chromatid pairing in wild-type and *rmi1* cells at two different chromosome loci: at a Tet operator locus located 35 kb from the centromere of chromosome 5 (*CEN5*) and another located 12.7 kb from *CEN4*. When the *CEN5* locus was monitored in nocodazole-arrested cells, 8% of M-phase wild-type cells had two GFP signal foci, whereas approximately 30% of M-phase *rmi1* cells had two GFP signals, indicating that *rmi1* cells, similar to *ctf18* cells, are defective in sister chromatid cohesion (Fig 2D, left panel). A similar result was obtained with the Tet operator at the *CEN4* locus (Fig 2D, right panel). When cells were arrested in G1 phase, the percentage of cells with two GFP signal foci was similar between wild-type and *rmi1* cells, excluding the possibility that the increase seen in M-phase-arrested *rmi1* cells was due to aneuploidy (Fig 2D).

To eliminate the possibility that the cohesion defect in *rmi1* cells was caused by premature destruction of the separin (Esp1) inhibitor Pds1, we monitored the levels of Pds1 in M-phase-arrested cells. We confirmed that Pds1 was present in similar amounts in *rmi1* cells showing two GFP signals and in wild-type cells (Fig 2C).

To investigate whether the *RMI1* mutation affects the recruitment of cohesin to the Tet operator locus, we carried out chromatin immunoprecipitation to examine the association of sister chromatid cohesion 1 (Scc1) at the uracil 3 (*URA3*) locus, where the Tet operator is integrated. Myc-tagged Scc1 was immunoprecipitated from extracts prepared from M-phase-arrested cells and the location of Scc1 was identified by performing PCR. We used the series of PCR primer pairs described by Lam *et al* (2006) to map Scc1 association over the entire *URA3* region

(Fig 2E). We found that Scc1-binding profiles were indistinguishable between *rmi1* and wild-type cells (Fig 2E), suggesting that Rmi1 is not involved in the recruitment of cohesin. Therefore, it appears that Rmi1 functions in the establishment of sister chromatid cohesion.

Rmi1 interacts physically and functionally with Sgs1 and Top3 (Chang *et al*, 2005; Mullen *et al*, 2005). Next, we examined whether Sgs1 or Top3 was also involved, along with Rmi1, in sister chromatid cohesion. We found that *top3* mutants, but not *sgs1* mutants, showed higher sensitivity to benomyl compared with wild-type cells (Fig 2A). In addition, sister chromatid cohesion was defective in *top3* mutants, but not in *sgs1* mutants (Fig 2D).

Deletion of *SGS1* or *RAD51* suppresses the cohesion defect

Top3 functions downstream of Sgs1 to resolve DNA substrates created by Sgs1. Most of the defects shown by *top3* mutants are suppressed by mutation of *SGS1* (Gangloff *et al*, 1994). Recent studies indicate that the growth defect and sensitivity to DNA-damaging agents of *rmi1* cells are also suppressed by *SGS1* deletion, suggesting that Rmi1 functions downstream of Sgs1, in a manner similar to Top3 (Chang *et al*, 2005; Mullen *et al*, 2005). As *sgs1* cells did not show benomyl sensitivity or a defect in sister chromatid cohesion (Fig 2), we examined whether these phenotypes were suppressed in *rmi1* and *top3* cells by deletion of *SGS1*. As shown in Fig 3A, deletion of *SGS1* suppressed the benomyl sensitivity of *rmi1* and *top3* cells. The cohesion defect in the mutant cells was also considerably suppressed by deletion of *SGS1* (Fig 3B). In addition, *rmi1top3* double mutants showed similar levels of benomyl sensitivity and cohesion defects to those of the corresponding single mutants, suggesting that Rmi1 and Top3 act at the same stage of cohesion establishment (Fig 3C,D).

Sgs1 functions downstream of Rad51 under certain conditions. Next, we asked whether deletion of *RAD51* also suppressed the cohesion defect in *rmi1* cells. As shown in Fig 3F, the cohesion defect in *rmi1* cells was suppressed by the disruption of *RAD51*, to a similar level as that seen in *rad51* cells. These results indicate that activation of a pathway involving Rad51 and Sgs1 results in sister chromatid cohesion by the functions of Top3 and Rmi1, and that dysfunction of Top3 or Rmi1 causes defects in cohesion. However, disruption of *RAD51* did not suppress the benomyl sensitivity of *rmi1* cells (Fig 3E), indicating that the cohesion defect does not necessarily correlate with benomyl sensitivity.

What then is the pathway involving Rad51 and Sgs1, which causes sister chromatid cohesion by the functions of Top3 and Rmi1? An attractive model involving Rad51, Sgs1 and Top3 was proposed by Liberi *et al* (2005). In this model, when the DNA replication fork encounters DNA lesions, a hemicatenane with double Holliday junctions is formed through the action of Rad51, and dissolved by Sgs1 and Top3, resulting in restoration of the replication fork (Liberi *et al*, 2005). Interpreting our results in the context of this model, Rmi1 and also Sgs1 and Top3 would be involved in the dissolution of double Holliday junctions. Indeed, the human homologue of Rmi1, BLAP75, stimulates dissolution of double Holliday junctions by BLM and Top3α (Raynard *et al*, 2006; Wu *et al*, 2006). Thus, Rmi1 together with Top3 might have a crucial role in coupling dissolution and cohesion.

The suppression of the cohesion defect of *rmi1* cells by disruption of *SGS1* or *RAD51* can be explained by the following model. Sgs1 and Rad51 generate recombination intermediates

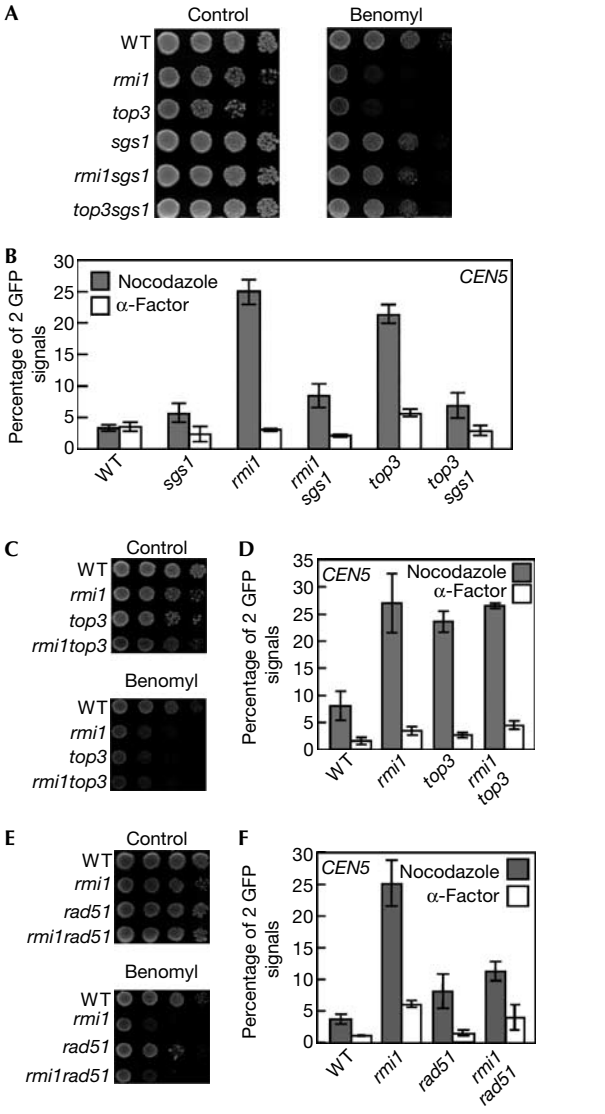

Fig 3 | Deletion of *SGS1* or *RAD51* suppresses cohesion defects in *rmi1* and *top3* cells. (**A**,**C**,**E**) Serial tenfold dilutions of log phase cultures of (**A**) wild-type (YPH1477), *rmi1* (YPH1477r1), *top3* (YPH1477t3), *sgs1* (YPH1477s1), *rmi1sgs1* (YPH1477r1s1) and *top3sgs1* (YPH1477t3s1) cells, (**C**) of wild-type (YPH1477), *rmi1* (YPH1477r1), *top3* (YPH1477t3) and *rmi1top3* (YPH1477r1t3) cells, and (**E**) of wild-type (YPH1477), *rmi1* (YPH1477r1), *rad51* (YPH1477r51) and *rmi1rad51* (YPH1477r1r51) cells were spotted onto growth plates containing 0, 20 (**A**,**E**) or 22 μg/ml (**C**) benomyl, incubated at 30 °C for 3 days and then photographed. (**B**,**D**,**F**) The same combination of cells in (**A**), (**C**) and (**E**) were used. Cells were arrested in M-phase with nocodazole or in G1 phase with α-factor and then fixed with paraformaldehyde. One hundred cells of each strain were scored for number of cells with two green fluorescent protein (GFP) signal foci. The data shown represent the average of three experiments. Bars indicate standard deviation. WT, wild type.

that require Top3 and Rmi1 for processing to establish cohesion. In the presence of Sgs1, the access of other factors to recombination intermediates is inhibited. When Sgs1 is absent, a structure-specific nuclease resolves the Holliday junctions, eliminating the

requirement for Top3 and Rmi1 in the establishment of sister chromatid cohesion. In the absence of Rad51, hemicatenanes with double Holliday junctions are not formed and the lesions are bypassed or repaired by systems that do not perturb the original sister chromatid cohesion.

In conclusion, we provide the first evidence, to our knowledge, indicating that Rmi1 and Top3 are involved in sister chromatid cohesion. Functional studies that explain the molecular mechanism linking Rmi1 and Top3 with cohesion, and confirm the validity of the above model are the focus of current and future efforts in our laboratory.

METHODS

Yeast strains and medium. The yeast strains used are listed in supplementary Table S1 online. We thank P. Hieter and V. Guacci for their generous gift of strains. The medium used for growth was described previously (Rose *et al*, 1990).

Flow cytometry, DNA staining and immunofluorescence. Flow cytometry, DNA staining and immunofluorescence were carried out as described previously (Branzei *et al*, 2002).

Spot assay. Log-phase cells grown in YPD medium were collected, washed once with distilled water, counted and diluted appropriately. Tenfold serial dilutions of cells (10^5, 10^4, 10^3 and 10^2 cells) were spotted onto YPD with or without benomyl. The plates were incubated at 30 °C for 2–4 days and then photographed.

Cohesion assay. Strains containing Tet repressor-GFP/Tet operator repeats were arrested in M phase or G1 phase by incubation with 15 μg/ml nocodazole and 5 μg/ml α-factor, respectively, for 5 h at 30 °C. Cells were then fixed by incubation with an equal volume of 4% paraformaldehyde for 30 min, washed once with SK (1 M sorbitol, 0.05 M K_2PO_4) and resuspended in 50 μl SK for cohesion assessment.

Pds1 assay. Immunostaining and western blotting of Pds1 were carried out as described previously (Mayer *et al*, 2004).

Chromatin immunoprecipitation. Log-phase cells expressing Myc-tagged Scc1 were arrested in M phase by incubation with 15 μg/ml nocodazole for 5 h. ChIP was carried out using the Myc antibody as described previously (Ogiwara *et al*, 2007).

Supplementary information is available at *EMBO reports* online (http://www.emboreports.org).

ACKNOWLEDGEMENTS

This work was supported by grants for Scientific Research and for Scientific Research on Priority Areas from the Ministry of Education, Culture, Sports, Science and Technology of Japan.

REFERENCES

Bennett RJ, Noirot-Gros MF, Wang JC (2000) Interaction between yeast *sgs1* helicase and DNA topoisomerase III. *J Biol Chem* **275:** 26898–26905

Branzei D, Seki M, Onoda F, Yagi H, Kawabe Y, Enomoto T (2002) Characterization of the slow-growth phenotype of *S. cerevisiae* Whip/Mgs1 Sgs1 double deletion mutants. *DNA Repair* **1:** 671–682

Chang M, Bellaoui M, Zhang C, Desai R, Morozov P, Delgado-Cruzata L, Rothstein R, Freyer GA, Boone C, Brown GW (2005) *RMI1/NCE4*, a suppressor of genome instability, encodes a member of the RecQ helicase/Topo III complex. *EMBO J* **24:** 2024–2033

Ellis NA, Groden J, Ye TZ, Straughen J, Lennon DJ, Ciocci S, Proytcheva M, German J (1995) The Bloom's syndrome gene product is homologous to RecQ heliases. *Cell* **83:** 655–666

Fabre F, Chan A, Heyer WD, Gangloff S (2002) Alternative pathways involving Sgs1/Top3, Mus81/Mms4, and Srs2 prevent formation of toxic recombination intermediates from single-stranded gaps created by DNA replication. *Proc Natl Acad Sci USA* **99:** 16887–16892

Fricke WM, Brill SJ (2003) Slx1–Slx4 is a second structure-specific endonuclease functionally redundant with Sgs1–Top3. *Genes Dev* **17:** 1768–1778

Gangloff S, McDonald JP, Bendixen C, Arthur L, Rothstein R (1994) The yeast type I topoisomerase Top3 interacts with Sgs1, a DNA helicase homolog: a potential eukaryotic reverse gyrase. *Mol Cell Biol* **14:** 8391–8398

Hanna JS, Kroll ES, Lundblad V, Spencer FA (2001) *Saccharomyces cerevisiae CTF18* and *CTF4* are required for sister chromatid cohesion. *Mol Cell Biol* **21:** 3144–3158

Ira G, Malkova A, Liberi G, Foiani M, Haber JE (2003) Srs2 and Sgs1–Top3 suppress crossovers during double-strand break repair in yeast. *Cell* **115:** 401–411

Kitao S, Shimamoto A, Goto M, Miller RW, Smithson WA, Lindor NM, Furuichi Y (1999) Mutations in *RECQL4* cause a subset of cases of Rothmund–Thomson syndrome. *Nat Genet* **22:** 82–84

Koshland DE, Guacci V (2000) Sister chromatid cohesion: the beginning of a long and beautiful relationship. *Curr Opin Cell Biol* **12:** 297–301

Lam WW, Peterson EA, Yeung MT, Lavoie BD (2006) Condensin is required for chromosome arm cohesion during mitosis. *Genes Dev* **20:** 2973–2984

Li R, Murray AW (1991) Feedback control of mitosis in budding yeast. *Cell* **66:** 519–531

Liberi G, Maffioletti G, Lucca C, Chiolo I, Baryshnikova A, Cotta-Ramusino C, Lopes M, Pellicioli A, Haber JE, Foiani M (2005) Rad51-dependent DNA structures accumulate at damaged replication forks in *sgs1* mutants defective in the yeast ortholog of *BLM* RecQ helicase. *Genes Dev* **19:** 339–350

Mayer ML, Gygi SP, Aebersold R, Hieter P (2001) Identification of RFC (Ctf18p, Ctf8p, Dcc1p): an alternative RFC complex required for sister chromatid cohesion in *S. cerevisiae*. *Mol Cell* **7:** 959–970

Mayer ML *et al* (2004) Identification of protein complexes required for efficient sister chromatid cohesion. *Mol Biol Cell* **15:** 1736–1745

Michaelis C, Ciosk R, Nasmyth K (1997) Cohesins: chromosomal proteins that prevent premature separation of sister chromatids. *Cell* **91:** 35–45

Mullen JR, Nallaseth FS, Lan YQ, Slagle CE, Brill SJ (2005) Yeast Rmi1/Nce4 controls genome stability as a subunit of the Sgs1–Top3 complex. *Mol Cell Biol* **25:** 4476–4487

Nasmyth K, Peters JM, Uhlmann F (2000) Splitting the chromosome: cutting the ties that bind sister chromatids. *Science* **288:** 1379–1385

Ogiwara H, Ui A, Enomoto T, Seki M (2007) Role of Elg1 protein in double strand break repair. *Nucleic Acids Res* **35:** 353–362

Raynard S, Bussen W, Sung P (2006) A double Holliday junction dissolvasome comprising BLM, topoisomerase IIIα, and BLAP75. *J Biol Chem* **281:** 13861–13864

Rose MD, Winston F, Hieter P (1990) *Methods in Yeast Genetics*. Cold Spring Harbor, NY, USA: Cold Spring Harbor Laboratory Press

Schmidt KH, Kolodner RD (2004) Requirement of Rrm3 helicase for repair of spontaneous DNA lesions in cells lacking Srs2 or Sgs1 helicase. *Mol Cell Biol* **24:** 3213–3226

Skibbens RV, Corson LB, Koshland D, Hieter P (1999) Ctf7p is essential for sister chromatid cohesion and links mitotic chromosome structure to the DNA replication machinery. *Genes Dev* **13:** 307–319

Strom L, Lindroos HB, Shirahige K, Sjogren C (2004) Postreplicative recruitment of cohesin to double-strand breaks is required for DNA repair. *Mol Cell* **16:** 1003–1015

Tong AH *et al* (2004) Global mapping of the yeast genetic interaction network. *Science* **303:** 808–813

Torres JZ, Schnakenberg SL, Zakian VA (2004) *Saccharomyces cerevisiae* Rrm3p DNA helicase promotes genome integrity by preventing replication fork stalling: viability of *rrm3* cells requires the intra-S phase checkpoint and fork restart activities. *Mol Cell Biol* **24:** 3198–3212

Uhlmann F (2004) The mechanism of sister chromatid cohesion. *Exp Cell Res* **296:** 80–85

Ui A, Satoh Y, Onoda F, Miyajima A, Seki M, Enomoto T (2001) The N-terminal region of Sgs1, which interacts with Top3, is required for complementation of MMS sensitivity and suppression of hyper-recombination in *sgs1* disruptants. *Mol Genet Genomics* **265:** 837–850

Ui A, Seki M, Ogiwara H, Onodera R, Fukushige S, Onoda F, Enomoto T (2005) The ability of Sgs1 to interact with DNA topoisomerase III is essential for damage-induced recombination. *DNA Repair* **4:** 191–201

Warren CD, Eckley DM, Lee MS, Hanna JS, Hughes A, Peyser B, Jie C, Irizarry R, Spencer FA (2004) S-phase checkpoint genes safeguard high-fidelity sister chromatid cohesion. *Mol Biol Cell* **14:** 1724–1735

Watt PM, Hickson ID, Borts RH, Louis EJ (1996) *SGS1*, a homologue of the Bloom's and Werner's syndrome genes, is required for maintenance of genome stability in *Saccharomyces cerevisiae*. *Genetics* **144:** 935–945

Weinert TA, Hartwell LH (1988) The *RAD9* gene controls the cell cycle response to DNA damage in *Saccharomyces cerevisiae*. *Science* **241:** 317–322

Wu L, Bachrati CZ, Ou J, Xu C, Yin J, Chang M, Wang W, Li L, Brown GW, Hickson ID (2006) BLAP75/RMI1 promotes the BLM-dependent dissolution of homologous recombination intermediates. *Proc Natl Acad Sci USA* **103:** 4068–4073

Yu CE *et al* (1996) Positional cloning of the Werner's syndrome gene. *Science* **272:** 258–262